

## Ellipsometry of micro-objects and structures

D. L. Lyutov\*, G. G. Tsutsumanova, S. C. Russev

*Department of Solid State Physics and Microelectronics, Faculty of Physics,  
St. Kliment Ohridski University of Sofia, 5 James Bourchier Blvd., BG-1164 Sofia, Bulgaria*

The conventional ellipsometry is very sensitive to changes of the surface in direction, normal to the surface of the specimen. The resolution in the plane of the surface is much lower – of the order of the width of the probe beam. For examination of micro-objects greater resolution is needed. In this work, construction and characterization of prototype of ellipsometric device with improved lateral resolution is presented. Its potential for local measurement of the ellipsometric angles is demonstrated and it is tested on different structures and micro-objects.

**Key words:** ellipsometry, micro-objects, lateral resolution

### INTRODUCTION

In recent years, the interest in research on microstructures and micro-objects has increased considerably. The conventional ellipsometry has very high sensitivity in direction normal to the surface – it is sensitive to submonoatomic changes of the surface. However its lateral resolution is much lower – it is limited by the width of the probe beam. There are techniques that improve the lateral resolution like Brewster angle microscopy [1–3], focusing ellipsometry [4, 5] and imaging ellipsometry [6–10], but the aim of most of them is acquiring image rather than measuring the ellipsometric parameters  $\psi$  and  $\Delta$ . Although quantitative measurements are possible with some of these techniques [10], their accuracy is lesser than that of the conventional ellipsometry. Our aim is to assemble ellipsometric devices with improved lateral resolution but to keep the accuracy of the measurement of the ellipsometric parameters  $\psi$  and  $\Delta$ . Two prototypes of such ellipsometric devices are presented in this work. They are tested on different samples dielectric, metal and semiconductor. The tests on micro-objects require objective with appropriate magnification. Therefore other tests are made to examine how the magnification of the optical system affects the ellipsometric measurement. Comparison is made between measurements on micro-objects and large surface of the same material by the conventional ellipsometry.

### EXPERIMENTAL SECTION

Two experimental setups, based on null type ellipsometer arrangement are made in this work. The two setups are distinguished by the position of the magnifying optical system. The two possible arrangements are polarization state generator/sample/optical system (objective)/polarization state detector (PSG-S-OS-PSD) and polarization state generator/sample/polarization state detector/optical system (objective) (PSG-S-PSD-OS). Each of them has its own advantages and drawbacks.

The first arrangement (PSG-S-OS-PSD) has the advantage that the objective is close to the sample and the resolution is greater but the objective itself changes the polarization and gives deviation in the measurement. In the second arrangement (PSG-S-PSD-OS) the objective does not change the polariza-

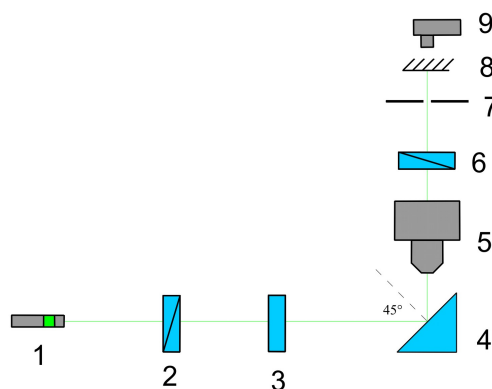


Fig. 1. Scheme of the first prototype arrangement (PSG-S-OS-PSD): 1 – laser; 2 – polarizer; 3 – compensator; 4 – sample on the micrometric table; 5 – objective; 6 – analyzer; 7 – aperture for selection of single object; 8 – screen; 9 – photo detector.

\* To whom all correspondence should be sent:  
d\_lyutov@phys.uni-sofia.bg

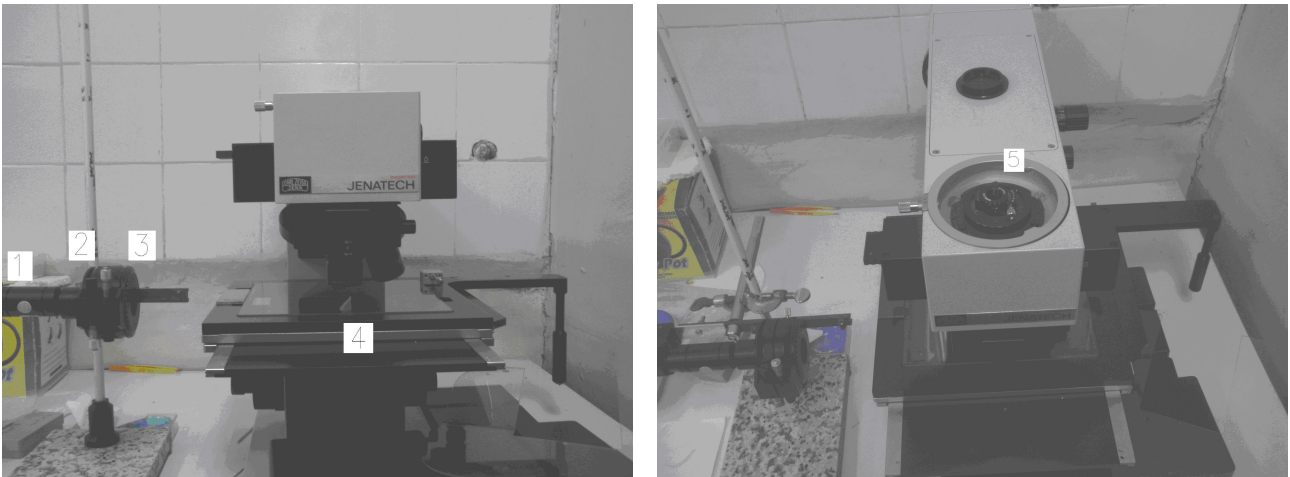


Fig. 2. Prototype (PSG-S-OS-PSD) viewed in front: 1 – laser; 2 – polarizer; 3 – compensator; 4 – sample and viewed from above: 5 – analyzer.

tion because it is after the polarization state detector and it does not change the conditions for the ellipsometric null.

The scheme of the PSG-S-OS-PSD prototype is shown in Fig. 1 and the construction – in Fig. 2. Microscope “Carl Zeiss”, light source, polarizer, compensator, analyzer and screen are used for the assembling of the first experimental setup. The light source is laser with wavelength  $\lambda = 532$  nm. The polarizer is type Glan-Thompson and the analyzer is made of dichroic polymer. The polarizer, compensator and analyzer can be rotated at arbitrary angle which allows four-zone measurement. The angle of incidence is fixed at  $45^\circ$ . The microscope’s x-y table allows lo-

calization of the micro-objects. Photo detector can be used for more accurate measurement of the minimum of the intensity instead to be determined visually at the screen. The numerical aperture and the resolution are the same as these of the microscope because the working distance is the same as in normal mode. So the resolution is approximately  $1 \mu\text{m}$ .

Conventional ellipsometer “Rudolf Research” and microscope “Carl Zeiss” are used for assembling the second experimental setup (PSG-S-PSD-OS) – Fig. 3.

Laser with wavelength  $\lambda = 532$  nm, polarizer Glan-Thompson, compensator, micrometric table for the sample, analyzer Glan-Thompson, movable optical system (Fig. 3), microscope system and screen or

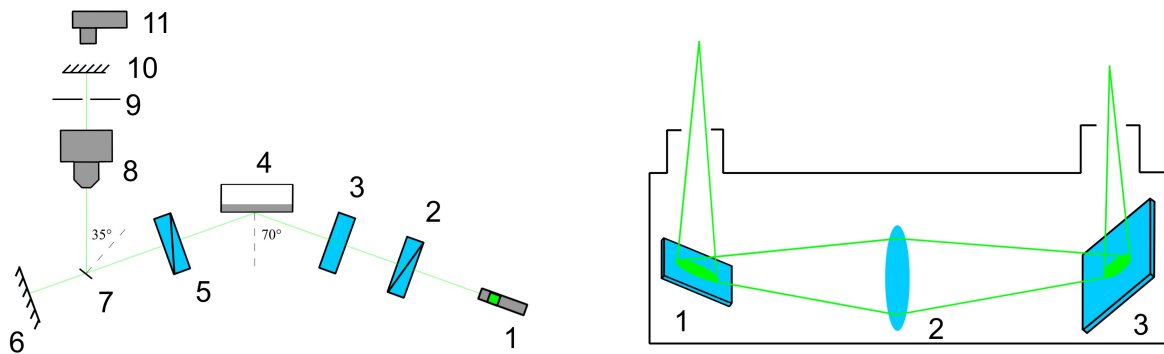


Fig. 3. *Left*: Scheme of the prototype with arrangement (PSG-S-PSD-OS): 1 – laser, 2 – polarizer, 3 – compensator, 4 – sample on micrometric table, 5 – analyzer, 6 – screen, 7 – movable optical system for relaying the image close to the objective of the microscope, 8 – optical system (objective), 9 – aperture for selection of single object, 10 – screen, 11 – photo detector. *Right*: Movable system in profile: 1,3 – mirrors, 2 – relay lens.

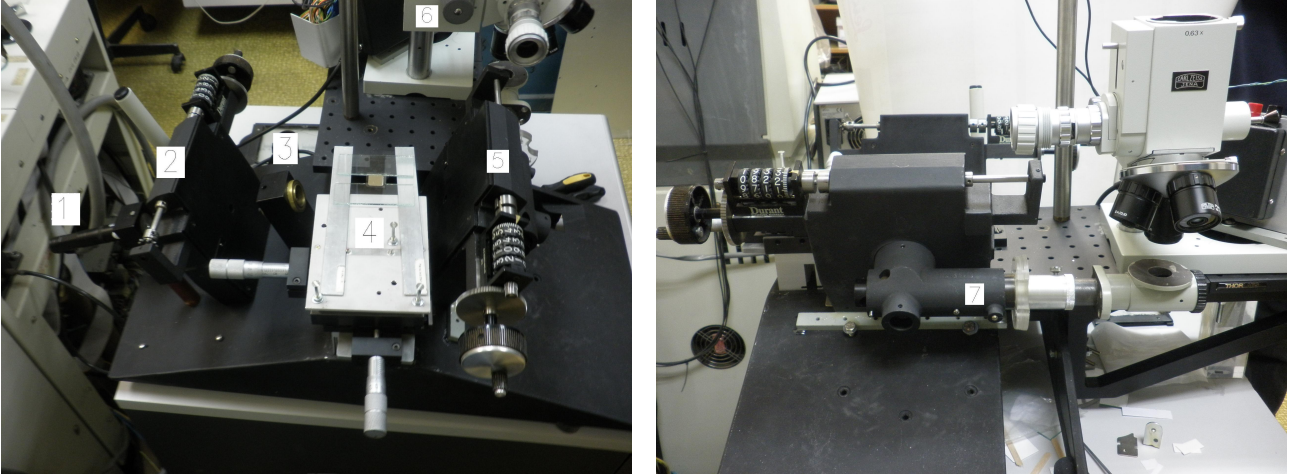


Fig. 4. Experimental setup with ellipsometer “Rudolf Research” and microscope “Carl Zeiss”. *Left*: Top view. 1 – laser, 2 – polarizer, 3 – compensator, 4 – x-, y- micrometric table, 5 – analyzer, 6 – microscope. *Right*: Side view. 7 – optical system used to relay the image close to the microscope.

photo detector are used in the second configuration. In this experimental setup, the polarizer and analyzer can be rotated at an arbitrary angle, but the compensator is fixed and only two zone measurements are possible. A possible improvement is adding azimuth indicator which will allow four zone measurements. The angle of incidence is  $70^\circ$  and is fixed. Pictures of the second experimental setup are shown at Fig. 4.

This setup can be used for conventional ellipsometric measurements by pulling out the optical system 7 (Fig. 4, right) and the intensity of the whole beam spot is minimized at the screen 6 (Fig. 3, left). If the system 7 is placed the beam is guided through microscope and the image is focused at the screen 10 (Fig. 3, left).

In this arrangement (PSG-S-PSD-OS) the objective is at long distance from the sample so the numerical aperture of the used relay lens is determining for the resolution of the whole system. The result is that the resolution is lower than that of the microscope. The resolution is determining for the minimal size of the objects which can be observed. Therefore it is estimated for this experimental setup.

The criterion for resolution of optical system is

$$r = \frac{1.22\lambda}{2n \sin(\theta)}, \quad (1)$$

where  $n$  is the refractive index of the medium,  $\lambda$  is the wavelength and  $\theta$  is the aperture angle. The refractive index of the air is  $n \approx 1$ , the wavelength of the laser is  $\lambda = 532nm$ ,  $\theta$  is determined from the distance from

the sample to the lens  $l = 200$  mm and diameter of the lens  $d = 20$  mm.

$$\sin(\theta) \approx \tan(\theta) = \frac{d}{2l} = \frac{20}{2 \times 200} = 0.05 \quad (2)$$

The resolution is

$$\begin{aligned} r &= \frac{1.22\lambda}{2n \sin(\theta)} = \frac{0.61\lambda}{\sin(\theta)} \\ &= 0.61 \times 532 \times 10^{-9} / 0.05 = 6.5 \mu\text{m}. \end{aligned} \quad (3)$$

## RESULTS

To determine their potential capabilities, null measurements are made with both experimental setups. The ellipsometric angles are calculated from the azimuth angles of the optical elements [11]:

$$\rho = -\tan A \left[ \frac{\tan C + \rho_C \tan(P - C)}{1 - \rho_C \tan C \tan(P - C)} \right] \quad (4)$$

where  $\rho$  is the ellipsometric ratio

$$\rho = \tan \psi e^{i\Delta} \quad (5)$$

and  $\rho_C$  is the ratio of coefficients of transmission between slow and fast axis of the compensator

$$\rho_C = T_C e^{i\Delta} \quad (6)$$

$P$ ,  $C$  and  $A$  are the azimuth angles of polarizer, compensator and analyzer. The uncertainty is estimated from the width of the minimum of the intensity.

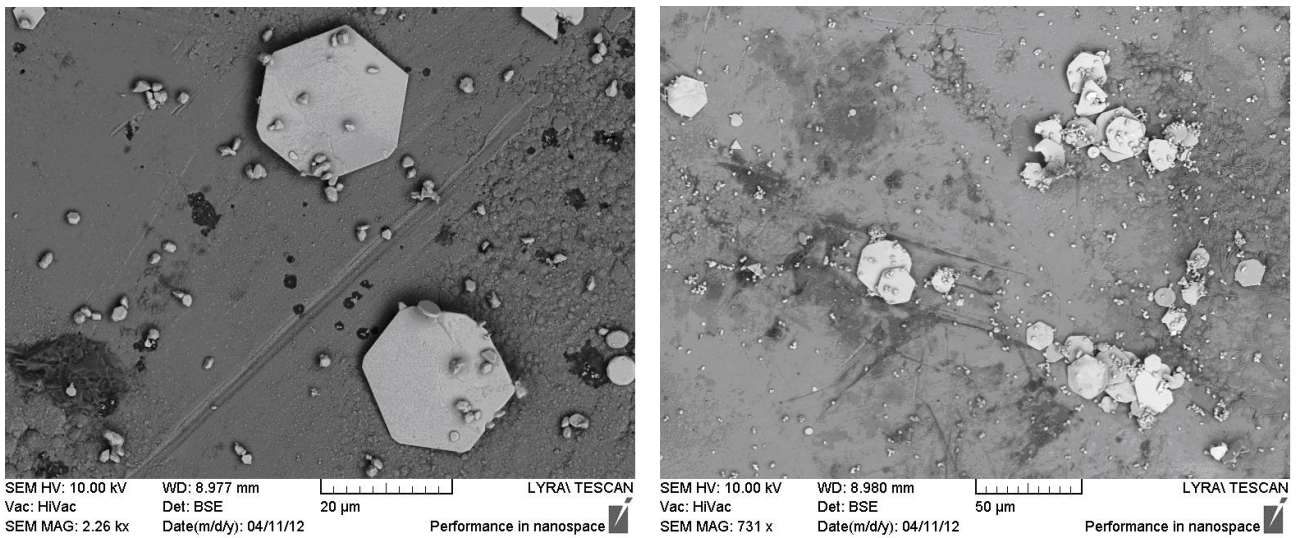


Fig. 5. Scanning electron microscope images of the Ag microparticles.

*Measurements with prototype (PSG-S-OS-PSD)*

Silver microparticles [12] with lateral dimensions in the range 10–20  $\mu\text{m}$  are used as test objects – (Fig. 5). Four-zone measurements were performed using microscope objective with magnification  $\times 10$ .

The measured values of the ellipsometric angles ( $\psi = 39.45^\circ \pm 1.44^\circ$  and  $\Delta = 160^\circ \pm 2.00^\circ$ ) differ from the calculated values for bulk silver ( $\psi = 44.84^\circ$  and  $\Delta = 156.50^\circ$  for refractive index  $N = 0.05 - 3.324i$  and wavelength  $\lambda = 521.5 \text{ nm}$  [13]). This can be caused by the effect of the optical system (the objective) which changes the polarization. The main advantage of this configuration (PSG-S-OS-PSD) is that

the intensity of the light reflected from micro-object is minimized so ellipsometric null is achieved. A good spatial resolution is attained – the size of the particle is 10  $\mu\text{m}$ .

*Measurements with prototype (PSG-S-PSD -OS)*

Measurements on samples made of three different materials are performed: glass K8, chrome (200 nm electron beam evaporation Cr layer on glass) and silicon (thickness 0.35 mm,  $\langle 111 \rangle$  orientation). Conventional ellipsometric measurements and measurements with magnification  $\times 5$ ,  $\times 10$  and  $\times 50$  are made to examine if the objective affects the measurement for each sample.

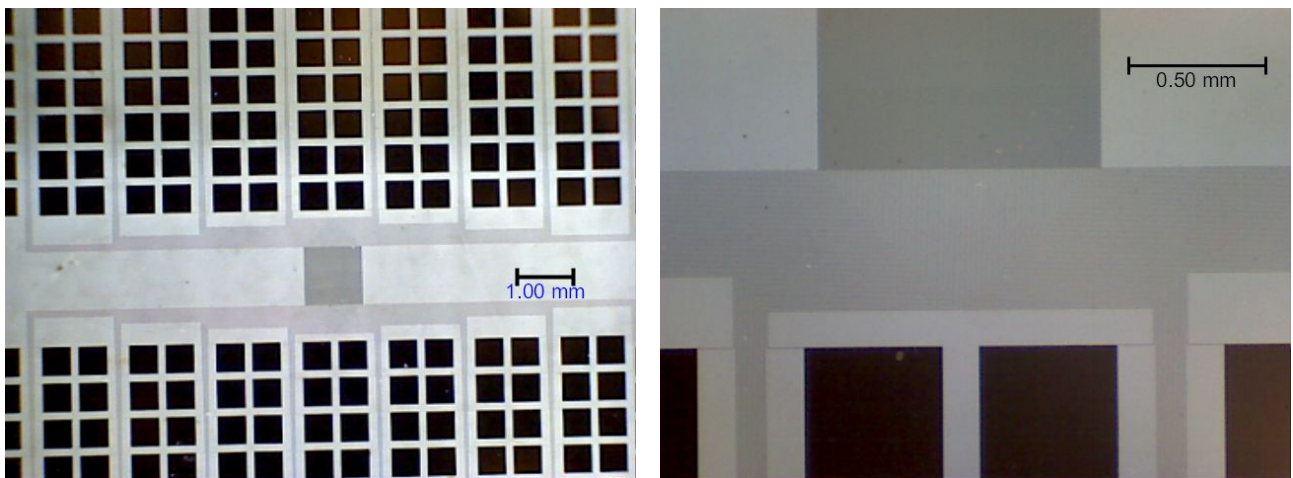


Fig. 6. Optical microscope image of the photolithographic mask No 1 at different magnifications. Squares are  $500 \times 500 \mu\text{m}$ .

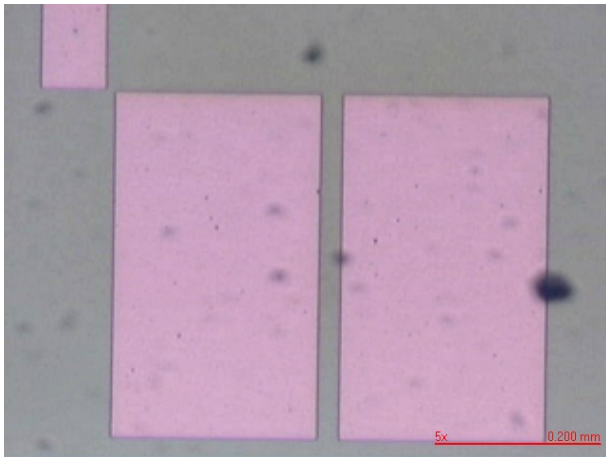


Fig. 7. Optical microscope image of the photolithographic mask No 2 with rectangle structures  $200 \times 400 \mu\text{m}$  and  $50 \times 100 \mu\text{m}$ .

$\psi$  and  $\Delta$  are measured on two photolithographic masks, labeled photolithographic mask No. 1 (Fig. 6) and photolithographic mask No. 2 (Fig. 7).  $\psi$  and  $\Delta$  are measured on photolithographic mask No 1 by conventional method on large surface, with objectives with magnification  $\times 5$ ,  $\times 10$  and  $\times 50$  and on  $500 \times 500 \mu\text{m}$  area with objective with magnification  $\times 50$ . Two regions of photolithographic mask No 2 (size  $200 \times 400 \mu\text{m}$  and  $50 \times 100 \mu\text{m}$ ) are measured. An attempt is made to measure  $\psi$  and  $\Delta$  on large area in photolithographic mask No2 but it is determined that the thickness of the layer is not the same on the whole surface. The results from these measurements are summarized in Table 1 and shown in Figs. 8 and 9.

Table 1. Ellipsometric angles measured on three different materials by conventional method and with objective with different magnification (configuration (PSG-S-PSD-OS))

Structure/magnification	$\psi$ [°]	$\Delta$ [°]
K8 conventional	$19.69 \pm 0.21$	$0.89 \pm 0.63$
K8 $\times 5$	$19.79 \pm 0.22$	$0.77 \pm 0.86$
K8 $\times 10$	$19.69 \pm 0.33$	$0.88 \pm 0.85$
K8 $\times 50$	$19.77 \pm 0.55$	$0.89 \pm 1.29$
Cr conventional	$26.99 \pm 0.29$	$113.23 \pm 0.86$
Cr $\times 5$	$27.03 \pm 0.40$	$113.65 \pm 0.78$
Cr $\times 10$	$27.12 \pm 0.29$	$113.51 \pm 0.78$
Cr $\times 50$	$27.13 \pm 0.42$	$113.25 \pm 1.13$
Si conventional	$12.74 \pm 0.28$	$167.62 \pm 0.76$
Si $\times 5$	$12.67 \pm 0.25$	$168.05 \pm 0.74$
Si $\times 10$	$12.69 \pm 0.25$	$167.62 \pm 0.96$
Si $\times 50$	$12.56 \pm 0.38$	$167.79 \pm 0.90$

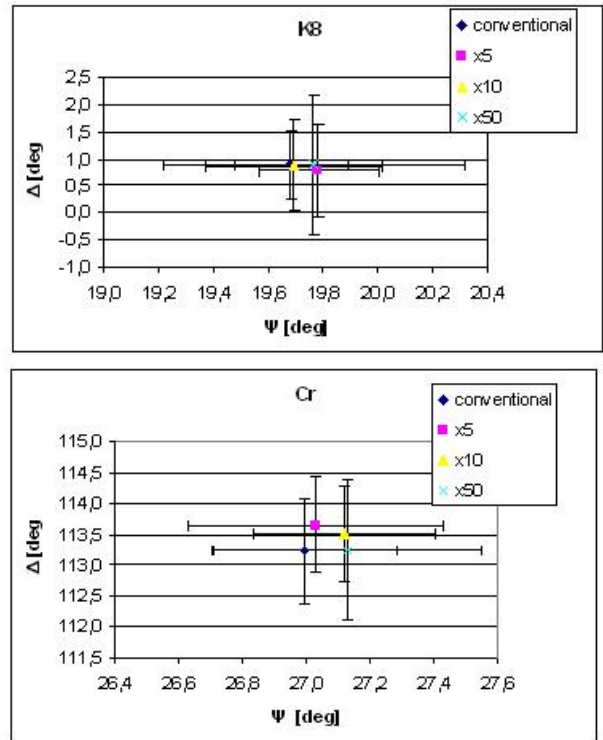


Fig. 8. Results attained for glass K8 and Cr with estimated uncertainty.

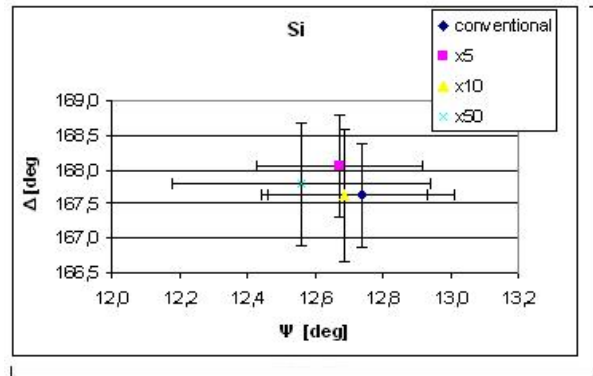


Fig. 9. Results attained for Si with estimated uncertainty.

The results from measurements on photolithographic mask No 1 (Table 2, Fig. 10, up) demonstrate that the variation of  $\psi$  and  $\Delta$  are in the range of the valued uncertainty. The uncertainty increases when the magnification increases. The uncertainty of  $\psi$  and  $\Delta$  measured on micro-object is greater than that of flat surface with the same magnification. This can be caused by scattering of light from the edges of the micro-object. The reached local measurement is of object with size  $500 \times 500 \mu\text{m}$ .

Table 2. 1 – results from conventional measurement; 2, 3 and 4 measurement on large area with objectives with magnification  $\times 5$ ,  $\times 10$  and  $\times 50$ , 5 – measurement on micro-object with size  $500 \times 500 \mu\text{m}$

Lithographic mask No 1		$\psi$ [deg]	$\Delta$ [deg]
1	Cr conventional	$31.22 \pm 0.19$	$50.44 \pm 0.68$
2	Cr $\times 5$	$31.22 \pm 0.24$	$50.57 \pm 0.59$
3	Cr $\times 10$	$31.24 \pm 0.41$	$50.27 \pm 0.73$
4	Cr $\times 50$	$31.14 \pm 0.27$	$50.75 \pm 0.66$
5	Cr $\times 50$ on micro-object	$31.33 \pm 0.51$	$50.34 \pm 1.20$

The results from measurement on photolithographic mask No 2 are shown in Table 3 and Fig. 10, down. The ellipsometric angles for objects with size  $200 \times 400 \mu\text{m}$  and  $50 \times 100 \mu\text{m}$  are in the range of the estimated uncertainty.

Table 3. Ellipsometric angles for lithographic mask No 2

$200 \times 400 \mu\text{m}$		$50 \times 100 \mu\text{m}$	
$\psi$ [deg]	$\Delta$ [deg]	$\psi$ [deg]	$\Delta$ [deg]
$14.09 \pm 0.67$	$28.73 \pm 1.54$	$14.25 \pm 0.98$	$29.30 \pm 1.88$

Example of minimizing the intensity on different objects is shown in Fig. 11. Under different conditions ellipsometric null is achieved on the object or in the background.

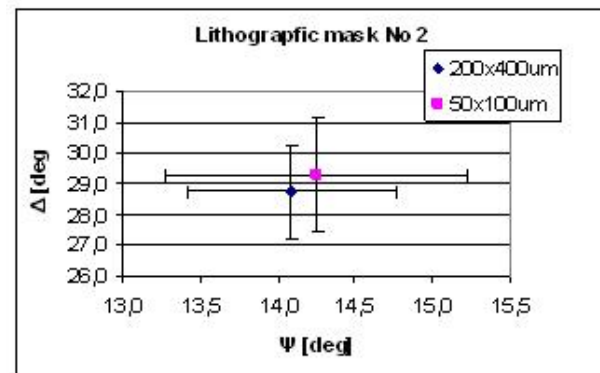
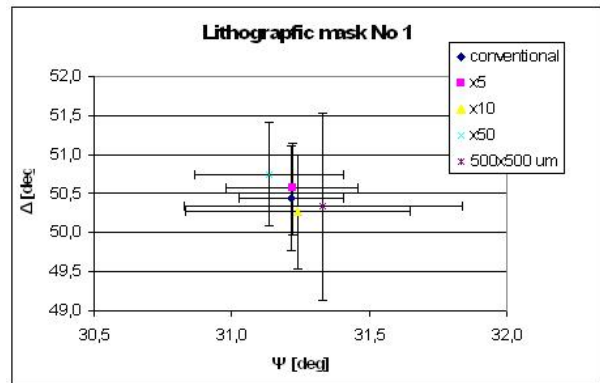


Fig. 10. Results for lithographic masks No. 1 and No. 2 with estimated uncertainty.

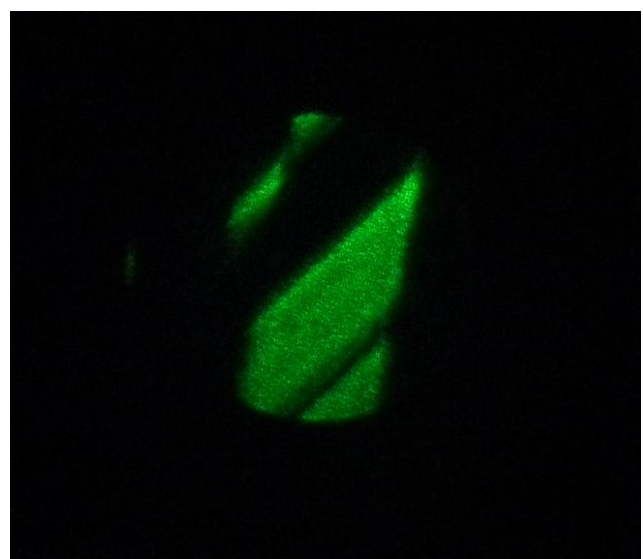
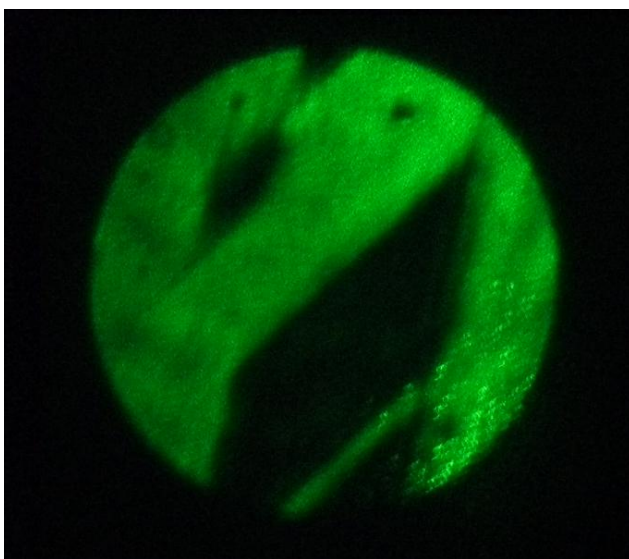


Fig. 11. Image of the photolithographic mask No 2, projected on the screen. **left**: the minimizing of the intensity is on metal surface. **right**: the minimizing of intensity is on the glass surface.

## CONCLUSIONS

Two prototypes of ellipsometric devices for micro-ellipsometry were made. They were tested on micro-objects and compared by conventional measurements on large surfaces of the same material. It is demonstrated that ellipsometric measurement can be performed on micro-objects with accuracy close to that of the conventional measurement.

Several improvements can be made. One of them is adding azimuth indicator to the compensator which will allow four-zone measurements. This will remove the errors caused by imperfections of the optical elements. Another improvement is using photo detector which will increase the accuracy of detecting the ellipsometric null. The experimental setup can also be used for imaging ellipsometry.

## REFERENCES

- [1] M. A. Cohen Stuart, R. A. J. Wegh, J. M. Kroon, E. J. R. Sudhölter, *Langmuir* **12**, 2863-2865 (1996).
- [2] Z. Kozarac, D. Moebius, M. T. Martin, *Water Res.* **34**, 1463–1472 (2000).
- [3] I. Kubo, S. Adachi, H. Maeda, and A. Seki, *Thin Solid Films* **393**, 80-85 (2001).
- [4] S.-H. Ye, Y. K. Kwak, S. H. Kim, H. M. Cho, Y. J. Cho, W. Chegal, D. G. Seiler, A. C. Diebold, R. McDonald, C. M. Garner, D. Herr, R. P. Khosla, E. M. Secula, “Development of a Focused-Beam Ellipsometer Based on a New Principle” in *AIP Conference Proceedings* **931**, 69–73 (2007).
- [5] G. D. Feke, D. P. Snow, R. D. Grober, P. J. de Groot, L. Deck, *Appl. Opt.* **37**, 1796–1802 (1998).
- [6] U. Wurstbauer, C. Röling, U. Wurstbauer, W. Wegscheider, M. Vaupel, P.H. Thiesen, D. Weiss, Dieter, *Appl. Phys. Lett.* **97**, 231901 (2010).
- [7] A. J. Choi, T. H. Ghong, Y. D. Kim, J. H. Oh, J. Jang, *J. Appl. Phys.* **100**, 113529-113529-5 (2006).
- [8] H. K. Pak, B. M. Law, *Rev. Sci. Instrum.* **66**, 4972-4976 (1995).
- [9] K. R. Neumaier, G. Elender, E. Sackmann, R. Merkel, *EPL (Europhysics Letters)* **49** 14 (2000).
- [10] L. Asinovski, D. Beaglehole, M. T. Clarkson, *Physica Status Solidi (a)* **205**, 764–771 (2008).
- [11] R. M. A. Azzam, N. M. Bashara, *Ellipsometry and polarized light*, North-Holland personal library, North-Holland Pub. Co. (1977).
- [12] D. L. Lyutov, K. V. Genkov, A. D. Zypkov, G. G. Tsutsumanova, A. N. Tzonev, L. G. Lyutov, S. C. Russev, *Mater. Chem. Phys.* **143**, 642–646 (2014).
- [13] P. B. Johnson, R. W. Christy, *Phys. Rev. B* **6**, 4370–4379 (1972).

## ЕЛИПСОМЕТРИЯ НА МИКРООБЕКТИ И СТРУКТУРИ

Д. Лютов, Г. Цуцуманова, Ст. Русев

Физически факултет, Софийски университет “Св. Климент Охридски”,  
ул. “Джеймс Баучер” №5, 1164 София, България

(Резюме)

Елипсометрията е бърз, безразрушителен и безконтактен метод за изследване на оптични свойства на обемни материали, тънки слоеве и многослойни структури. Този метод намира приложение в много области като изследването на твърдотелни структури, образуването на слоеве върху твърда или течна повърхност, микроелектрониката, химията и биологията.

Едно от основните предимства на този метод е, че има висока точност и е много чувствителен към изменения на повърхността. Конвенционалната елипсометрия има тази чувствителност по направление нормално на повърхността на образеца. Разделителната ѝ способност по повърхността на образеца е малка – от порядъка на милиметри. За изследванията на микрообекти е необходима значително по-добра разделителна способност.

В тази работа е представена конструкцията и характеризирането на прототип на елипсометрична апаратура с подобрена странична разделителна способност с възможност за локално измерване на елипсометричните ъгли и тестването ѝ върху различни структури и микрообекти.